JOURNAL OF GEOPHYSICAL RESEARCH, VOL. 115, A02212, doi:10.1029/2009JA014217, 2010

Click Here for Full Article

THEMIS observations of substorms on 26 February 2008 initiated by magnetotail reconnection

Z. Y. Pu,[1] X. N. Chu,[1] X. Cao,[1] V. Mishin,[2] V. Angelopoulos,[3] J. Wang,[1] Y. Wei,[1] Q. G. Zong,[1] S. Y. Fu,[1] L. Xie,[1] K.-H. Glassmeier,[4,5] H. Frey,[6] C. T. Russell,[3] J. Liu,[3] J. McFadden,[6] D. Larson,[6] S. Mende,[6] I. Mann,[7] D. Sibeck,[8] L. A. Sapronova,[2] M. V. Tolochko,[2] T. I. Saifudinova,[2] Z. H. Yao,[9] X. G. Wang,[9] C. J. Xiao,[9] X. Z. Zhou,[3] H. Reme,[10] and E. Lucek[11]

Received 6 March 2009; revised 4 September 2009; accepted 29 September 2009; published 26 February 2010.

[1] On 26 February 2008, the THEMIS satellites observed two substorms that occurred at about 0405 and 0455 UT. Angelopoulos et al. (2008) made a comprehensive study of the second event. In this paper we display detailed features of the two substorms with emphasis on the first. In both substorms, a distinct auroral intensification occurred during the earliest stage of onset, about 1 to 2 min after midtail reconnection began. This initial intensification was weak and localized and thus had the signatures of a pseudobreakup. In both substorms, a second, major intensification occurred next in the substorm onset sequence, followed by rapid and extensive poleward expansion. This second intensification had the features of the major expansion onset and was nearly coincident with observations of earthward flows and magnetic dipolarization in the near-Earth tail. During the growth phase of the two substorms, open magnetic flux accumulated in the polar cap; in the expansion/recovery phase the polar cap open flux was quickly reduced. These observations are in agreement with the assertion that tail reconnection initiates the initial pseudobreakup and the ensuing major expansion and releases and transports energy to eventually cause near-Earth dipolarization and the expansion phase onset of these two substorms.

Citation: Pu, Z. Y., et al. (2010), THEMIS observations of substorms on 26 February 2008 initiated by magnetotail reconnection, *J. Geophys. Res.*, *115*, A02212, doi:10.1029/2009JA014217.

1. Introduction

[2] Magnetospheric substorms have long been the focus of solar-terrestrial physics. The main unsolved issue is the mechanism that triggers the substorm expansion onset. A number of working models have been proposed; the near-Earth current disruption (NECD) model [e.g., *Lui*, 1996] and the near-Earth neutral line (NENL) model [e.g., *McPherron*, 1991; *Baker et al.*, 1996; *Baumjohann*, 2002] are among the most popular. In the NECD model, local instabilities [*Lui et al.*, 1990] cause current disruption (CD) at $X \sim -(8–10)\ R_E$, leading to dipolarization and current wedge formation; the CD region then expands tailward during the substorm expansion phase. The NENL model assumes that magnetic reconnection (MR) occurs in the region of $-20 > X > -30\ R_E$, producing the tailward moving plasmoid and earthward bursty bulk flow. The earthward flows transport magnetic flux and energy toward the near-Earth region to cause substorm onset. Besides, the synthesis scenario of MR and CD [*Pu et al.*, 1999, 2001; *Zhang et al.*, 2007] suggests that flow braking might yield conditions favorable for instabilities near the inner edge of the plasma sheet, causing substorm onset. In addition, substorms have been showed to often initiate with two steps: an initial onset (of a pseudobreakup) and a major onset (of the expansion phase) [*Nakamura et al.*, 1994; *Mishin et al.*, 2000, 2001; *Baker et al.*, 2002; *McPherron*, 2004]. The substorm onset timeline should provide a reference frame for organizing substorm onset phenomenology, thereby resolving the debate about substorm onset triggers.

[1]School of Earth and Space Sciences, Peking University, Beijing, China.
[2]Institute of Solar-Terrestrial Physics, Russian Academy of Sciences, Irkutsk, Russia.
[3]IGPP, UCLA, Los Angeles, California, USA.
[4]Instiute of Geophysics and Extraterrestrial Physics, Technical University of Braunschweig, Braunschweig, Germany.
[5]Max Planck Institute of Solar System Research, Katlenburg-Lindau, Germany.
[6]Space Sciences Laboratory, University of California, Berkeley, California, USA.
[7]Department of Physics, University of Alberta, Edmonton, Alberta, Canada.
[8]NASA GSFC, Greenbelt, Maryland, USA.
[9]School of Physics, Peking University, Beijing, China.
[10]Centre d'Etude Spatiale des Rayonnements, Toulouse, France.
[11]Blackett Laboratory, Imperial College London, London, UK.

Copyright 2010 by the American Geophysical Union.
0148-0227/10/2009JA014217$09.00

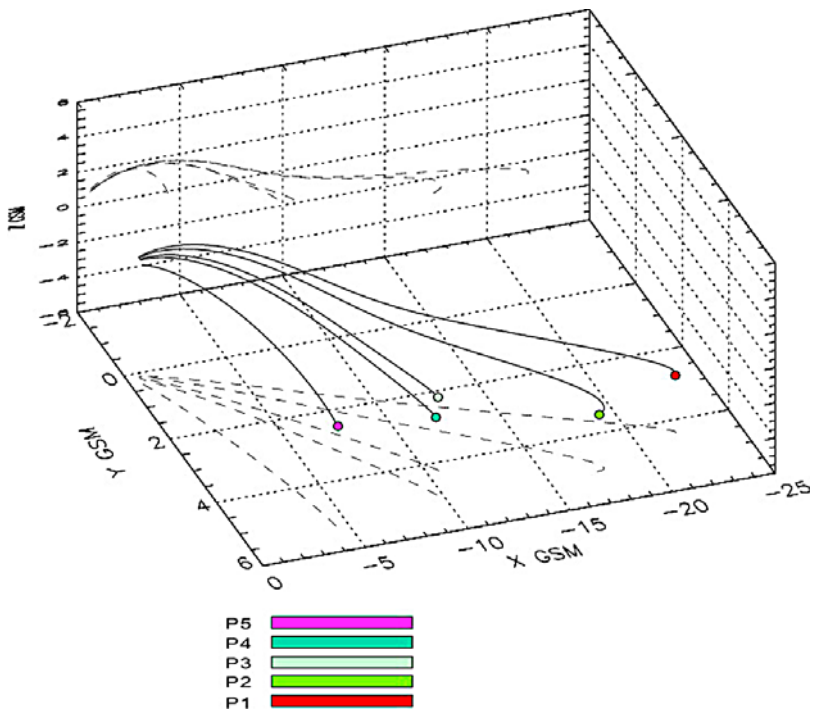

Figure 1. Positions of THEMIS probes in the GSM coordinates at 0400 UT with representative field lines based on the T-96 magnetic field mode [*Tsyganenko*, 1995].

[3] The THEMIS mission [*Angelopoulos*, 2008] was designed to resolve the NECD versus NENL controversy by employing five satellites and ground-based all-sky aurora imagers and magnetometers to observe substorm onset time history. The five probes were put into near-equatorial orbits with periods that are multiples of each other to determine the onset and evolution of substorm instability. In some cases, THEMIS observations suggest that MR in the midtail plasma sheet triggers substorm activities [e.g., *Runov et al.*, 2008]. The explosive process responsible for substorm onset is characterized by fast unloading of magnetic energy in the midtail [*Sergeev et al.*, 2008]. On the other hand, the measurements supporting substorm initiation by instabilities in the near-Earth plasma sheet have also been reported [e.g., *Liang et al.*, 2008]. Recently, *Angelopoulos et al.* [2008] studied timing and the causal relationship in the substorm event that occurred at ~0455 UT on February 26, 2008 using THEMIS in situ and ground-based measurements. They reported that midtail MR was observed at least 2 min before auroral substorm expansion, and about 3 min before near-Earth CD, and concluded that these results demonstrate that substorms are likely initiated by tail MR. The February 26, 2008 event has attracted attention in the substorm community [*Lui*, 2009; *Angelopoulos et al.*, 2009; *Zhou et al.*, 2009].

[4] In fact, there were two substorms with expansion phase onsets at about 0405 UT and 0455 UT on 26 February 2008. During the two events, the THEMIS satellites were all in/near the plasma sheet. *Angelopoulos et al.* [2008] made a comprehensive study of the second case. In this paper we present detailed features of the two substorms with emphasis on the former. We show that two auroral intensifications occurred during the earliest stage of the two substorms; the first, weak intensification appeared about 1–2 min immediately after the midtail MR onset, and the second, major intensification occurred within about one min when earthward flows and magnetic dipolarization were observed in the near-Earth tail. During the growth phase of the two substorms, the polar cap open magnetic flux accumulated; while in the expansion/recovery phase the polar cap open flux was quickly released. The accumulated and released open fluxes were both considerably less than in moderate substorms. It is thus very likely that weak tail MR resulted in the two small substorms observed on 26 February 2008.

[5] The paper is organized in the following manner: in section 2 we describe the data set used in the study; section 3 presents detailed observations; sections 4 and 5 discuss substorm timing and its relationship with tail MR; and section 6 gives a brief summary.

2. Data Set and Instruments

[6] From 0330 to 0530 UT on 26 February 2008, the THEMIS probes were located in/near the plasma sheet and aligned along the Sun-Earth line. In this study, we use the 3 s spin-integrated ion data from THEMIS/ESA [*McFadden et al.*, 2008] and magnetic field data from THEMIS/FGM [*Auster et al.*, 2008]. The auroral images are obtained from the THEMIS ground-based array of 20 all-sky imagers (ASIs) with a time resolution of 3 s and spatial resolution of 1 km [*Mende et al.*, 2008]. The ground-based magnetic field data are acquired from 21 THEMIS fluxgate magnetometers (GMAGs) [*Russell et al.*, 2008]. These GMAGs measure the magnetic field with 0.01 nT resolution at 2 samples/s. The auroral electrojet (AE) index is calculated from these

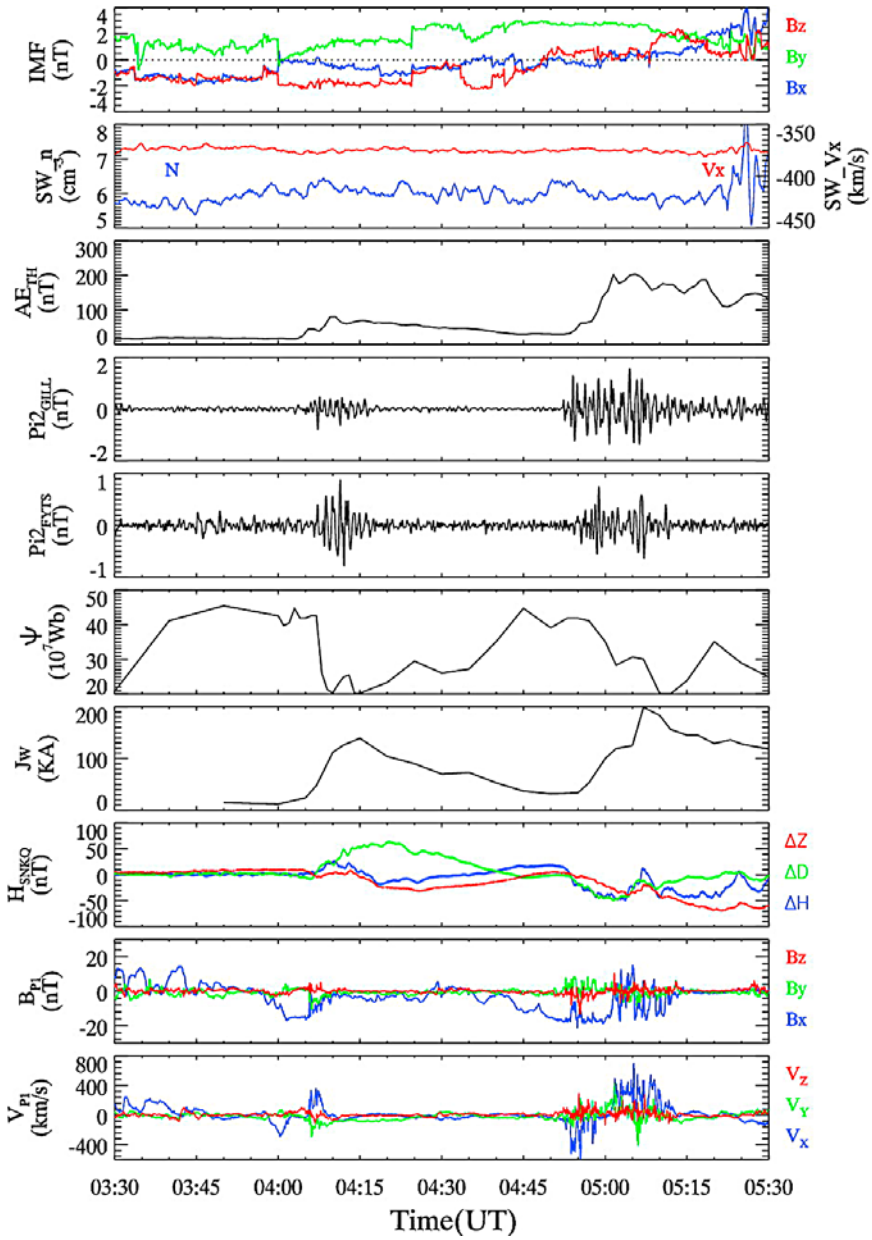

Figure 2. Two hour (0330–0530 UT) observations of two substorms on 26 February 2008. Shown are the IMF in front of the dayside bow shock measured by Cluster 3; the simultaneously measured X component of the solar wind velocity V_x and the solar wind number density N; the AE index obtained based on the magnetic field measurements of 21 THEMIS fluxgate magnetometers (GMAGs); Pi2 pulsation at the high-latitude GILL station (66.18°N, 332.78°E); Pi2 pulsations at the midlatitude FYTS (55.765°N, 35.281°W) station; the polar cap magnetic flux Ψ created by dayside reconnection calculated based on magnetic field measurements from 109 ground-based stations at magnetic latitudes $\Phi > 40°$; the westward electrojet current Jw obtained based on the magnetic field measurements from 27 stations around the northern hemisphere auroral zone; the three geomagnetic components at the SNAQ station; the magnetic field and flow velocity observed by THEMIS/P1.

GMAGs measurements. In addition, magnetic field measurements from 109 ground-based stations at magnetic latitudes $\Phi > 40°$(not shown in the paper) are used to estimate the polar cap magnetic flux Ψ employing the MIT2 technique [*Mishin*, 1990; *Mishin et al.*, 1997, 2001, and references therein]. Data from 27 of those stations distributed around the northern hemisphere auroral zone are applied to calculate the westward auroral electrojet current Jw. During the 2 h interval of interest, the four Cluster (C1-C4) spacecraft stayed in the near-Earth solar wind ($X \sim 17R_E$). Four second spin-integrated observations of magnetic field and ions from C3 are adopted as a monitor of

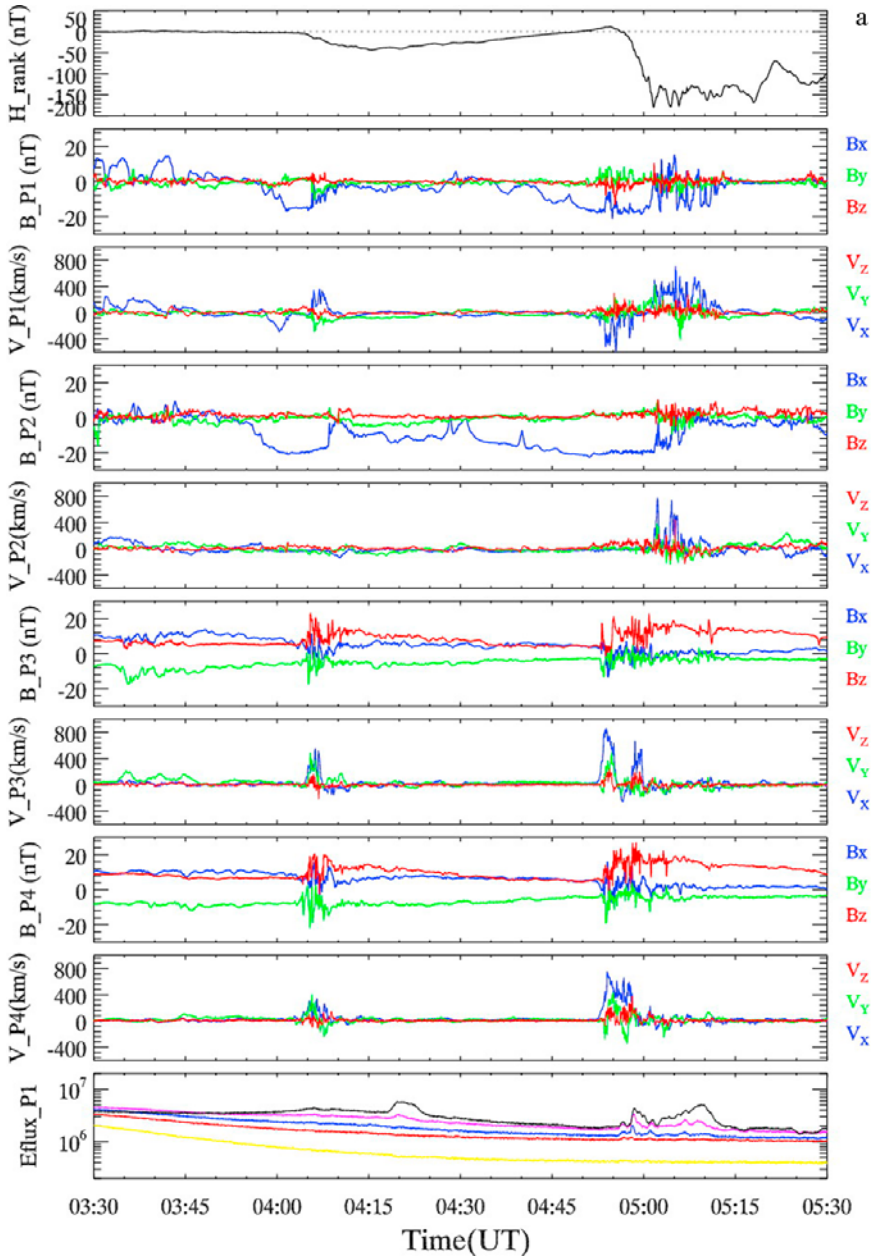

Figure 3. (a) Magnetic field and flow measurements of four THEMIS probes during the time period of (0330–0530 UT). Shown are plots of the geomagnetic H component at the RANK station and the magnetic field and plasma velocity measured by P1, P2, P3 and P4. (b) Magnetic field and flow measurements of four THEMIS probes during the 10 min time interval of (0357–0407 UT). The first and second panels show the THEMIS AE index and geomagnetic H component at the RANK station, respectively. The format is the same as in Figure 3a.

solar wind conditions. The GSM coordinates and geomagnetic latitude and longitude are used throughout the paper for displaying spacecraft positions and locations of ground-based auroral imagers and magnetometers, respectively.

3. Observations

3.1. Overview of Observations

[7] Figure 1 shows a 3-D view of THEMIS spacecraft positions at ~0400 UT with the projection onto the X-Z plane in the GSM coordinates. The magnetic field lines are drawn based on the T96 magnetospheric model [*Tsyganenko*, 1995]. All THEMIS satellites were located in or near the plasma sheet with P1 at (−21.9, 4.35, −2.72) R_E, P2 at (−17.40, 5.03, −2.88) R_E, P3 at (−10.60, 4.21, −1.84) R_E, P4 at (−9.77, 4.88, −1.61) R_E and P5 at (−4.48, 5.28, −0.16) R_E. Figure 2 shows 2 h (0330–0530 UT) observations of the IMF in front of the dayside bow shock, number density N and the X component of the solar wind velocity V_x, THEMIS AE index, Pi2 pulsation at the high-latitude

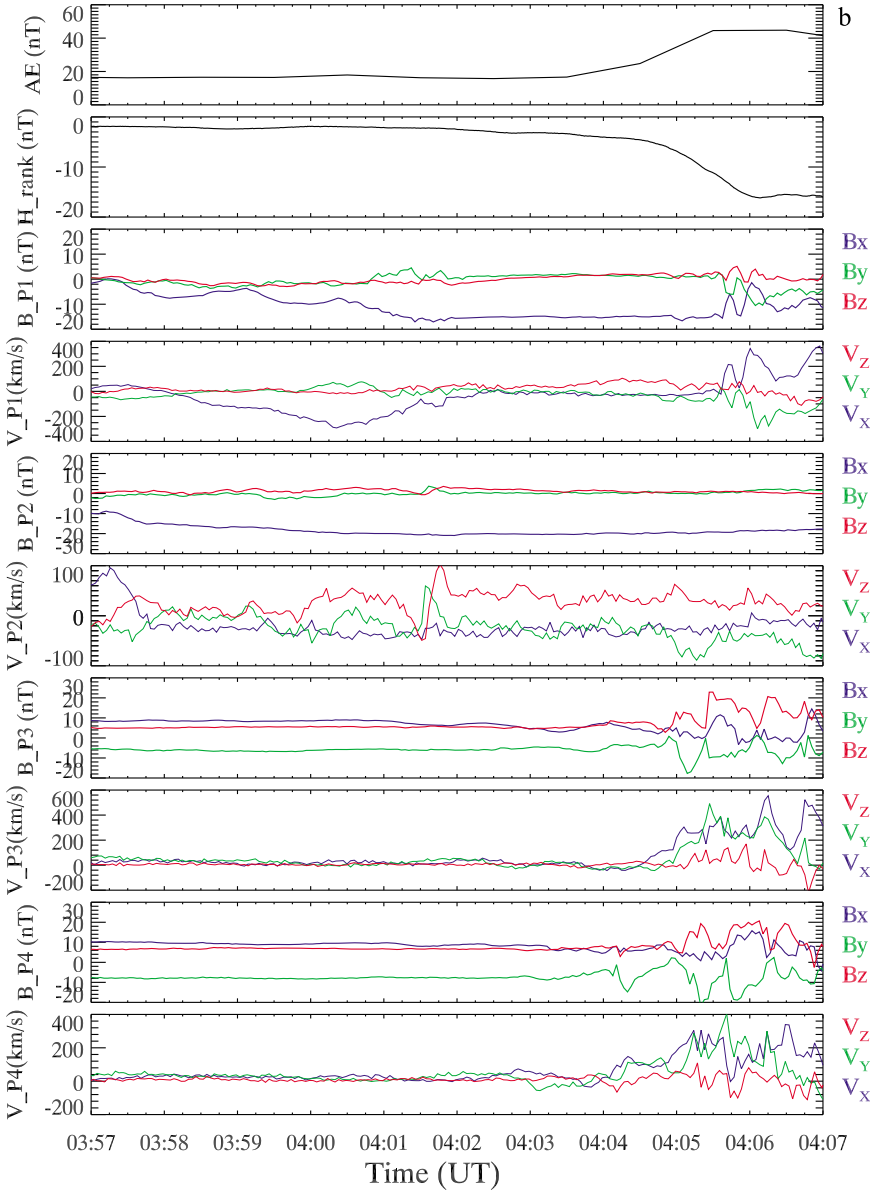

Figure 3. (continued)

GILL (66.18°N, 332.78°E) and midlatitude FYTS (55.765° N, 35.281°W), polar cap magnetic flux Ψ, westward electrojet current Jw, H component excursion at the SNAQ station (66.45°N, 356.99°E), magnetic field and flow velocity observed by THEMIS/P1. It is seen that the IMF B_Z remains negative until ~0448 UT with $|B_z| < 2$ nT and that solar wind N and V_x remain essentially unchanged. Figure 2 indicates that two substorm dipolarization/expansions took place at ~0405 and ~0455 UT. Closely associated with each dipolarization/expansion are enhancement of the AE index and Jw current, rising and falling of the open flux Ψ, a burst of Pi2 pulsation and a negative H excursion. It is quite evident that two sets of substorm expansion phase activities occurred separately during this 2 h period. Figure 3a shows the magnetic field and flow measurements of four THEMIS probes during the same time interval as in Figure 2. Plotted are the three geomagnetic components at the RANK station (72.41°N, 335.74°E), the magnetic field and plasma velocity of P1, P2, P3 and P4. It is clear that P1 encounters two independent flow reversals, and P3 and P4 observe two near-Earth dipolarization events following the arrival of earthward flows. Figure 3b plots the measurements of P1, P2, P3 and P4 during the 10 min interval from 0357:00 UT to 0407:00 UT. As mentioned above, all THEMIS data used in drawing Figures 2, 3a, and 3b are with 3 s time resolution. For ease of comparison with the ground-based measurements, we have shown the THEMIS AE and the H component of the magnetic field at RANK in the first and second panels of Figure 3b, respectively.

[8] *Angelopoulos et al.* [2008] have shown explicitly the initial auroral phenomena of the 0455 UT substorm at GILL. We will display in more detail the auroral activities of both

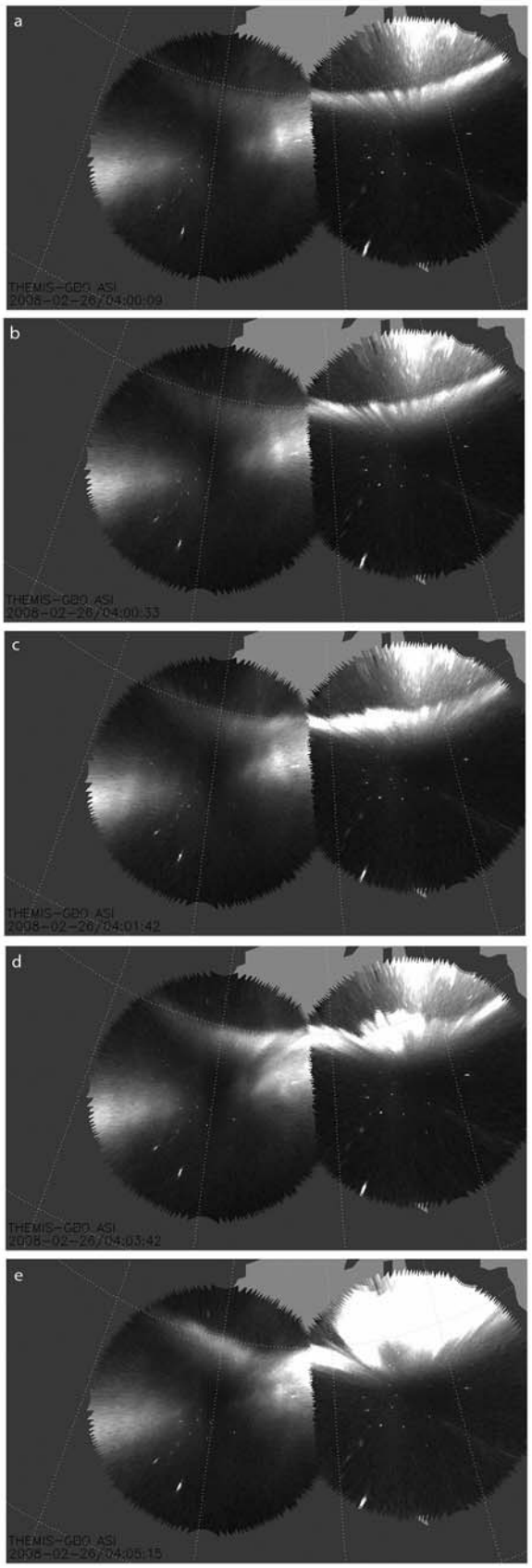

substorms in sections 3.2 and 3.3. It is worthwhile to mention that the auroral brightenings/expansions in the 0405 UT substorm appeared approximately 1 h earlier than those in the 0455 UT substorm and disappeared before the second substorm started its growth phase (see below).

3.2. The ~0405 UT Substorm

[9] A relatively stable auroral arc extended across the sky from GILL to SNKQ prior to the 0405 UT substorm. The auroral arc first started to intensify at 0400:21 UT at SNKQ and began a slight poleward expansion at 0401:21 UT. A second, stronger auroral intensification began at 0403:30 UT closer to midnight and rapidly/extensively expanded poleward at 0404:30 UT. The arc continued to brighten and expand afterward. We regard the first brightening as the initial intensification and the second brightening/expansion as the major auroral intensification/expansion of this event. Figure 4 illustrates the auroral arcs at SNKQ (right) (66.45° N, 356.99°E) and GILL (left) at five selected times: 0400:09 UT (before the initial intensification), 0400:33 UT (after the initial intensification), 0401:42 UT (after the first, local expansion), 0403:42 UT (after the major intensification) and 0405:15 UT (after the major expansion). A negative H-bay started at 0404:30 UT at RANK and arrived at a maximum of 44 nT at ~0415 UT. The THEMIS AE index also rapidly increased at 0404:30 UT. High-latitude GILL and midlatitude FYTS (55.76°N, 35.28°W) magnetometers recorded Pi2 onset at ~0402 UT and ~0406 UT, respectively. The GILL and FYTS pulsations arrived at a maximum of 1.0 nT at ~0411 UT and 1.7 nT at ~0411 UT, respectively. Ψ rapidly decreased from 42.54 × 10^7Wb at ~0407 UT to 20.22 × 10^7Wb at ~0415 UT. The westward auroral electrojet current Jw increased from 48 kA at ~0405 UT to 139 kA at ~0415 UT. In addition, at (−4.48, 5.28, −0.16) R_E P5 observed a weak energy-dispersed ion injection of 50–200 keV ions near the midnight geosynchronous altitude (not shown).

[10] In the meantime, the THEMIS spacecraft first located in the inner and midtail found evidence of midtail MR. THEMIS/P1 at (−21.9, 4.35,−2.72) R_E stayed in the dense and hot plasma sheet for 1 h, meeting earthward ion flows (~100–240 km/s). At 0358:27 UT, a tailward flow with a maximum speed of ~300 km/s and negative B_z started at P1 location. Meanwhile, the midtail plasma sheet was getting thinner, the spacecraft then moved toward the southern lobe. Beginning at 0405:16 UT, the flow became earthward with V_x ~ 400 km/s and positive B_z; see Figure 3b. According to the classical MR picture, this reversal of V_x and B_z implies a nearby crossing of the MR region from the tailward side to the earthward side [*Phan et al.*, 2000]. Furthermore, we have projected the measured magnetic field and velocity vectors into the current sheet coordinated system (L, M, N) (not shown here), where L, M and N represent the direction

Figure 4. Auroral brightening of the ~0405 UT substorm at (right) SNKQ and (left) GILL at five selected times: (a) 0400:09 UT (before the initial intensification), (b) 0400:33 UT (after the initial intensification), (c) 0401:42 UT (after the first, local expansion), (d) 0403:42 UT (after the major intensification), and (e) 0405:15 UT (after the major expansion).

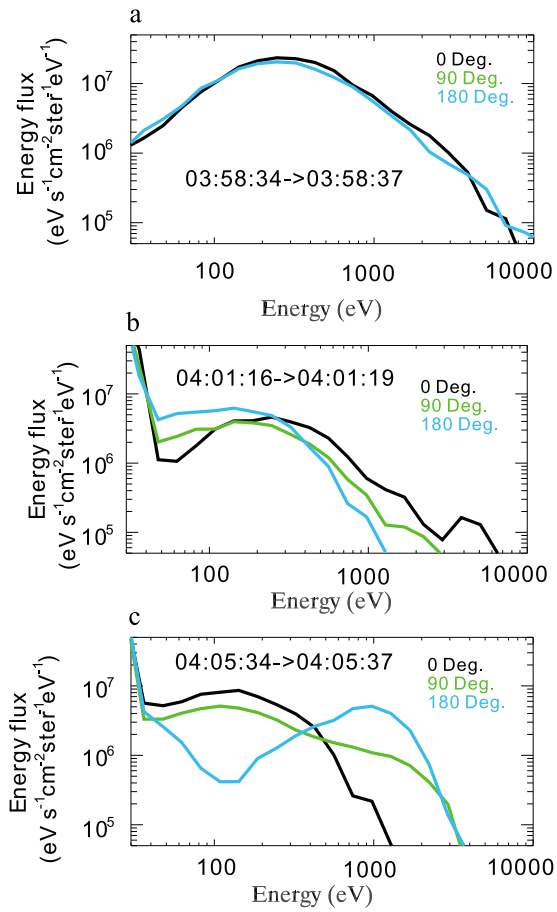

Figure 5. Bidirectional anisotropies of energetic electrons associated with Hall effect observed by P1. (a) The first P1 observation of electron bidirectional anisotropy averaging from 0358:34 UT to 0358:37 UT, when P1 was tailward of the reconnection site. (b) A typical electron bidirectional anisotropy averaging from 0401:16 UT to 0401:19 UT, when P1 was in the tailward outflow region close to the separatrix. (c) A typical electron bidirectional anisotropy averaging from 0405:34 UT to 0405:37 UT, when P1 had passed through the separatrix moving into the earthward outflow region.

of maximum, intermediate and minimum variation of the magnetic field, respectively [*Sonnerup and Scheible*, 1998], and the angle between positive N and the Z axis is less than 90° so that N is normal to the current sheet upward. In Figure 3b it is shown that while V_x (V_L) and B_z reverse their signs and B_x (B_L) remains negative, B_y (B_M) changes from positive to negative. This is in agreement with the fact that the spacecraft was encountering the Hall-quadrupole magnetic field near the diffusion region of ongoing MR [*Arzner and Scholer*, 2001; *Øieroset et al.*, 2001; *Pu et al.*, 2005], and that the MR site was retreating from the earthward side of P1 to the tailward side. Moreover, *Nagai et al.* [2001] have shown that when a spacecraft encounters the MR region, it sees field-aligned accelerated electrons flowing out near the separatrix. The associated electron bidirectional anisotropy provides an additional evidence of ongoing MR which has been regarded as a good indicator for in situ MR observations [e.g., *Øieroset et al.*, 2001; *Deng et al.*, 2004; *Owen et al.*, 2005; *Manapat et al.*, 2006; *Nakamura et al.*, 2006; *Angelopoulos et al.*, 2008]. This appears to be of particular importance when the plasma sheet is thinned. Two events on 26 February 2008 we studied are just the case where P1 was originally away from the central current sheet [*Angelopoulos et al.*, 2009]. We have analyzed the P1 measurements of the electron bidirectional anisotropy during the period of ~0356 UT to ~0407 UT. From 0356:01 UT to 0358:31 UT as the spacecraft stayed deep in the tailward outflow region, no anisotropy was seen. From 0358:34 UT to 0401:46 UT when P1 came toward the tailward side separatrix and detected tailward bulk flow and negative B_x and B_z, higher-energy (200–4000 eV) electrons were found to stream mostly tailward (PA ~ 0°) with a higher flux, while lower-energy (10–100 eV) electrons were seen to stream mostly earthward (PA ~ 180°) with a lower flux. Later from 0401:49 UT to 0405:13 UT when the spacecraft entered the inflow region detecting northward inflow, no bidirectional anisotropy was observed. Further later from 0405:16 UT to 0408:04 UT when P1 was passing through the earthward side separatrix and moved into the earthward outflow region, it was found that higher-energy (200–4000 eV) electrons were streamed mostly earthward (PA ~ 180°) with a higher flux, whereas lower-energy (10–100 eV) electrons were streamed mostly tailward (PA ~ 0°) with a lower flux. Figure 5a shows the first observation of a weak electron bidirectional anisotropy averaging from 0358:34 to 0358:37 UT. Figures 5b and 5c show more pronounced anisotropies averaging from 0401:16 to 0401:19 UT (as P1 was in the tailward outflow region not far from the separatrix) and averaging from 0405:34 to 0405:37 UT (as P1 had moved into the earthward outflow region near the separatrix), respectively. This is consistent with the picture that the spacecraft observed the tailward retreating Hall structure near the MR diffusion region [see *Nagai et al.*, 2001, Figure 1]. Auxiliary material Figures S1–S13 show this retreat process in more detail.[1] It is of interest to note also that as the MR region moved to the tailward side of P1, the spacecraft encountered earthward flow, along with a decrease of B_x and an increase of B_z. This dipolarization signature was obviously caused by flux transport/pileup associated with ongoing retreating MR. All these results strongly suggest that MR occurred earthward of P1 at least at or before 0358:34 UT.

[11] Nevertheless, measurements by P2 at (−17.40, 5.03, −2.88) R_E show neither the clear Hall-B_y field, nor the related electron bidirectional anisotropy. The position of P2 (further away from the central current sheet and midnight) could explain these deviations from the typical Hall signatures of collisionless MR. Note that P2 did not see flow and flux transport/dipolarization signatures, either. One feature, however, that supports the occurrence of MR is the prominent thinning of the tail current sheet [*Arzner and Scholer*, 2001] starting at ~0557:45 UT, which was best seen by the spacecraft as a strong decrease in the B_x component of the magnetic field. Therefore from P1 and P2

[1]Auxiliary materials are available in the HTML. doi:10:1029/2009JA014217.

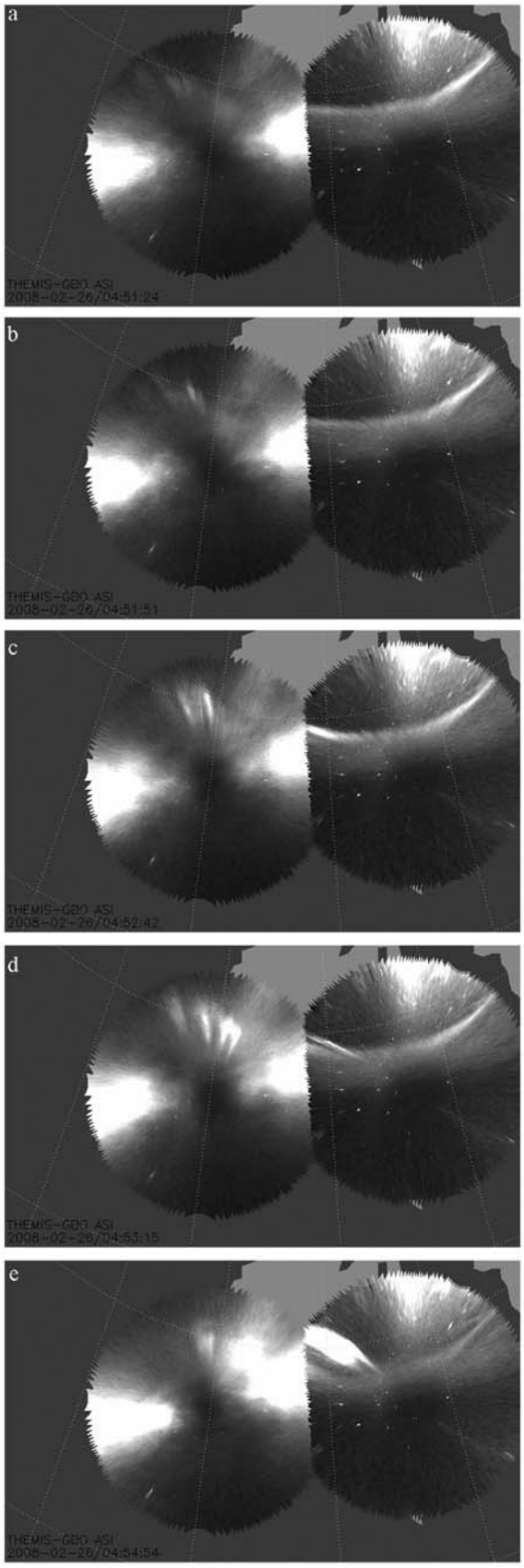

measurements it is reasonable to expect that a MR event took place at $X > -21.9$ R_E at least at or before 0358:34 UT.

[12] The onset of earthward flow was first detected by P4 at (−9.77, 4.88, −1.61) R_E at 0404:16 UT, accompanied by a highly fluctuated magnetic field. P3 at (−10.60, 4.21, −1.84) R_E observed the flow arrival at 0404:48 UT, 32 s later than P4. A sudden increase in B_z, which we interpret as magnetic dipolarization, occurred at 0404:48 UT at P4 and 0404:51 UT at P3. No bidirectional anisotropy similar to Figure 5c is found during dipolarization.

3.3. The ~0455 UT Substorm

[13] *Angelopoulos et al.* [2008] carefully studied the substorm at ~0455 UT. The electron bidirectional anisotropy of collisionless MR was observed by P1 at 0450:28 UT; later P2 also observed MR signatures at 0450:38 UT. The first auroral intensification occurred at 0451:39 UT at GILL and slightly expanded poleward at 0452:21 UT. P3 saw earthward flow at 0452:27 UT and dipolarization at 0453:05 UT. The high-latitude Pi2 began at 0452:00 UT and midlatitude Pi2 at 0453:05 UT. Meanwhile, with a careful inspection one can see that the ASI at SNKQ observed the second stronger intensification at 0453:03 UT and subsequent rapid/extensive expansion at 0453:48 UT. Afterward the arc continued to brighten and expand. As in the previous case, we refer to the first, weak brightening as initial auroral intensification and the second brightening/expansion as major auroral intensification/expansion of this event. Figure 6 shows the auroral activities at SNKQ (right) (66.45°N, 356.99°E) and GILL (left) at five selected times: 0451:24 UT (before the initial intensification), 0451:51 UT (after the initial intensification), 0452:42 UT (after the first, limited expansion), 0453:15 UT (after the major intensification) and 0454:54 UT (after the major expansion).

[14] In Figure 2 one sees that the negative H-bay at RANK started at ~0454 UT and arrived at a maximum of 178 nT at ~0501 UT. The THEMIS AE index arose at ~0454 UT; Jw increased from ~0455 UT to a maximum of 199 kA at 0507 UT; Ψ decreased from 41.83×10^7Wb at ~0455 UT to 23.85×10^7Wb at ~0515 UT. In addition, P5 observed an energy-dispersed ion injection of 50–200 keV ions near the midnight geosynchronous altitude (not shown).

[15] It is worthwhile to note that the auroral arc in the 0405 UT substorm had moved equatorward and become quiet by ~0435 UT, and AE, Jw, Pi2 and H excursion all had reduced to very small values at ~0435 UT. Therefore, the 0405 UT and 0455 UT substorms manifest two separate events. Moreover, Ψ started to increase again at ~0435 UT, reached the peak at ~0453 UT, and then reduced two minutes later. Thus the MR onset at 0450:03 UT and the 0455 UT substorm activities seem to be related not to the

Figure 6. Auroral activities of the ~0455 UT substorm at (right) SNKQ and (left) GILL at five selected times: (a) 0451:24 UT (before the initial intensification), (b) 0451:51 UT (after the initial intensification), (c) 0452:42 UT (after the first, limited expansion), (d) 0453:15 UT (after the major intensification), and (e) 0454:54 UT (after the major expansion).

Table 1. Time Sequence of Signatures of the 0405 UT Substorm

Event	Observed Time (UT)	Time Delay (s)
Start of tailward flow with $B_z < 0$ at P1	0358:29	
Reconnection effects (electron-Hall) at P1	0358:34	0
First auroral intensification	0400:21	107
First auroral expansion onset	0401:21	167
High-latitude Pi2 onset at GILL	~0402	~206
Second (major) auroral intensification	0403:30	296
Earthward flow onset at P4	0404:16	342
Earthward flow onset at P3	0404:48	374
Second (major) auroral expansion onset	0404:30	356
Negative H excursion at RANK	0404:30	356
Rapid increase of THEMIS AE	0404:30	356
Dipolarization at P4	0404:48	374
Dipolarization at P3	0404:51	377
Enhancement of westward electrojet current Jw	~0405	~386
Midlatitude Pi2 onset at FYTS	~0406	~446

0405 UT substorm, but rather to reaccumulation and rerelease of magnetic flux in the tail lobes after that event.

4. Time History and Causality of Substorms

[16] *Angelopoulos et al.* [2008] have illustrated the time history of the ~0455 UT substorm activities [see *Angelopoulos et al.*, 2008, Table 1]. The initial auroral intensification appeared 96 s after the inferred MR onset (or 71 s after the MR effects at P1) and 48 s ahead of earthward flow at P3. Therefore, as the authors suggested, the initial brightening cannot be caused by the near-Earth flux pileup of MR flow; rather, the MR generated kinetic Alfven waves and their accelerated electrons might explain the observations [*Angelopoulos et al.*, 2008]. On the other hand, the major intensification and major expansion of the auroral arcs occurred 36 and 81 s after the flow onset at P3, respectively. Moreover, both dipolarization at P3 and midlatitude Pi2 started 38 s following the flow onset at P3, and the rapid increase of THEMIS AE, enhancement of Jw and high-latitude negative H-bay began both about one min later. Thus, as *Angelopoulos et al.* [2008] noted, flux pileup and substorm current wedge (SCW) formation may be responsible for the near-Earth dipolarization and major onset of the expansion phase.

[17] Now we turn to the timing of the ~0405 UT substorm. The bidirectional anisotropy of Hall electrons at P1 (at 0358:34 UT) implies that MR occurred earthward of P1 at least at or before 0358:34 UT. One hundred and seven seconds after P1 detected the electron bidirectional anisotropy, the SNKQ ASI observed the initial auroral brightening at 0400:21 UT. High-latitude Pi2 pulsation took place 99 s later at ~0402 UT. At 0403:30 UT the ASI at SNKQ observed the major auroral intensification. P4 and P3 observed the onset of earthward flow at 0404:16 UT and 0404:48 UT, respectively. The major auroral expansion, the rapid increase of THEMIS AE and the high-latitude negative H-bay occurred at 0404:30 UT, as well. At nearly the same time P4 and P3 detected magnetic dipolarization at 0404:48 UT and 0404:51 UT, respectively. Immediately after that at ~0505 UT Jw started to enhance. About one minute later at ~0406 UT the midlatitude Pi2 pulsation began. These substorm timings are summarized in Table 1. Note that the time resolution associated with THEMIS measurements in Table 1 is 3 s.

[18] It is easy to find that the time history of the ~0405 UT substorm is similar to that of the ~0455 UT substorm in two respects. First, the initial auroral brightening appears around two minutes immediately after midtail MR, followed promptly by Pi2 pulsation at high-latitude stations. Using the T96 magnetospheric model [*Tsyganenko*, 1995], we projected P1 and P2 locations at 0405 UT to the ionosphere and found that the probe foot points lie within 0.5 h of the meridians of SNKQ and GILL. We thus infer that the midtail MR near $\sim X \sim -20\ R_E$ (possibly through the related kinetic Alfven waves and their accelerated electrons) initiated the initial auroral brightening of the ~0405 UT substorm, as in the case of ~0455 UT substorm suggested by *Angelopoulos et al.* [2008]. Second, the major intensification and major expansion of auroral arcs, magnetic dipolarization at P4 and P3, rapid increase of the THEMIS AE index, the enhancement of Jw and the beginning of the high-latitude negative H-bay were all observed within about one minute. More interestingly, all these expansion phase signatures started concurrently within about one minute of the onset of earthward flow at P4 and P3. A reasonable interpretation would be that all these activities shared a common source: the SCW formation associated with the flow braking [*Shiokawa et al.*, 1997, 1998; *Pu et al.*, 1999, 2001; *Baumjohann*, 2002]. This appears to be in agreement with the scenario that the earthward flows caused by midtail MR transport magnetic flux and energy to eventually cause the near-Earth substorm expansion onset [*Baker et al.*, 2002; *Cao et al.*, 2008]. Note that the MR event detected by P1 at ~0358 can be the cause of the major auroral brightening and dipolarization at P4 and P3 only if the signal propagation speed was much lower than the local Alfven speed. As shown in Figure 3b, the peak of the flow at P1 was just about 300 km/s, considerably lower than the local Alfven speed. In addition, in this event P3 and P4 may not be at the best position to detect the flow braking/SCW. For instance, P4 observed the onset of earthward flow and magnetic dipolarization 26 s and 3 s earlier than P3, respectively, although the location of P4 was about one R_E closer to the Erath than P3 (mostly in the X direction). Besides, one more minute delay of midlatitude Pi2 at FYTS could be due to that the station was somewhat away from the foot point of the SCW/CD location.

[19] It is worth noticing that the timing and causality of these two substorms strongly support the two-step scenario of substorm initiation [*Nakamura et al.*, 1994; *Mishin et al.*, 2000, 2001; *Baker et al.*, 2002; *McPherron*, 2004]. Multiple intensifications are a common feature of substorms [*Rostoker et al.*, 1980]. If these occur before the onset of the expansion phase, they are called pseudobreakups [*Koskinen et al.*, 1993; *Nakamura et al.*, 1994; *Mishin et al.*, 2000; *Ge et al.*, 2008]. Pseudobreakups are characterized by week auroral arcs that are short-lived and quite confined in latitude. Some pseudobreakups also have signatures of highly localized dipolarization without CD expansion [*Ohtani et al.*, 1993]. *Nakamura et al.* [1994] and *Mishin et al.*

[2000, 2001] suggested that substorms often have two distinct onsets. The first (named the initial onset) manifests the start of pseudobreakups. The second (called the major onset) represents the beginning of the expansion phase. During the expansion phase, auroral arcs expand significantly poleward and west-eastward and dipolarization/SCW evolve globally. Obviously, in two events studied in this paper, the first and second auroral brightenings indicate the initial and major substorm onsets, respectively. Furthermore, the polar cup open flux can be represented as the sum $\Psi = \Psi_1 + \Psi_2$, where Ψ_2 is the quasi-permanent part of Ψ, determined by MIT2 data for quite conditions before the substorm, and Ψ_1 is a variable part flux controlled by the IMF [*Mishin et al.*, 2001]. It has been known that the balance between dayside MR and nightside tail lobe MR (TLR) determines the amount of the variable polar cap flux Ψ_1 [*Cowley and Lockwood*, 1992] and that TLR of open field lines provides most of the flux and energy required for fully developed substorms [*Baker et al.*, 1996]. In the two events under consideration, it is determined with the MIT2 data that $\Psi_2 \approx 20.0 \times 10^7$ Wb. Rapid drop of Ψ/Ψ_1may then serve as an indication of TLR and evolution of the expansion phase. *Russell* [2000] and *Mishin et al.* [2000, 2001] thus proposed that the initial onset/pseudobreakups correspond to MR of the closed field lines in the plasma sheet (PSR); while at the major onset/beginning of the expansion phase, MR has evolved to open field lines in the lobes. Figure 2 shows that in the first and second event under consideration, Ψ/Ψ_1 started to rapidly decrease at ~0407 UT and ~0455 UT, about 3 and 2 min later than the major auroral brightening, respectively. Thus in these two substorms the initiation of the expansion phase might be related to either the TLR of open field lines while dayside MR was continuing to transport magnetic flux into the polar caps, or to the PSR of closed field lines followed very soon by TLR. In either case TLR was operating to support most energy dissipated during the expansion phase. Apparently, the aforementioned features of the two events strongly support the two-step initiation scenario of substorms.

5. Reconnection and Substorm Intensity

[20] In the literature, some authors regarded substorm activities as low and moderate if AE < 300 nT and the maximum AE ~ 500 nT, respectively [e.g., *Speiser et al.*, 1996; *Immel et al.*, 1997]. In Figure 2 one sees that the AE index maximums during the two events were ~80 nT and 203 nT. The highest Jw current in the two substorms reached 139 kA and 199 kA, much less than (500–1000) kA for moderate substorms [*Mishin et al.*, 2008]. The amplitudes of two negative H-bay were ~40 nT and ~178 nT, comparable to (100–300) nT in low-intensity substorms [*Kamide and Akasofu*, 1974; *Lui et al.*, 1976]. With such low substorm-related signatures, both events should be referred to as weak substorms.

[21] In view of both the NENL paradigm and the synthesis scenario of MR and CD, substorm intensity is virtually determined by the amount of flux and energy released by TLR. It is then reasonable to expect that the MR processes initiating the two substorms would be weak. There are two commonly used methods to estimate the MR rate: measuring the tangential electric field along the MR line, or the ratio of the inflow velocity V_{in} to the asymptotic Alfven speed V_A [*Priest and Forbes*, 2000]. Here we apply the latter approach based on measurements of P1. The key issue is to subtract the flapping effects from the observed Z component of the flow velocity. Supposing that MR is symmetric with respect to the upside and downside of the current sheet, in the MR rest frame of reference the plasma velocity would then contain no Z component at the center of the current sheet. We take the average of V_z measured as $|B_x| < 2$ nT to be the flapping velocity. For the 0455 event, the flapping V_{z0} is calculated as ~18.4 km/s. The mean Z component of plasma velocity $\langle V_z \rangle$ in the inflow region is ~47.8 km/s, thus V_{in} should be $\langle V_z \rangle - V_{z0} \sim 29.4$ km/s. The asymptotic V_A may also be obtained with the magnetic field and plasma density in the inflow region. With observed $\langle |B| \rangle = 17$ nT and $\langle N \rangle = 0.15 \sim 0.25$ cm^{-3}, V_A can be estimated at ~(750–970) km/s. These results give a low limit of a fast MR rate of ~(0.030–0.038). A similar approach leads to an MR rate of ~(0.04–0.05) for the 0405 event.

[22] Low intensity substorms and weak MR seem to be closely associated with the relatively smaller amounts of Ψ_1 created by dayside MR and $\Delta\Psi_1$ released by tail lobe MR during substorm expansion. The maximum Ψ_1 during the both events were ~22.0×10^7 Wb in both substorms, substantially lower than ~$(40–60) \times 10^7$ Wb for moderate substorms [*Pu et al.*, 2006; *Boakes et al.*, 2009]; the released fluxes $\Delta\Psi_1$ in the two events were ~22.0×10^7 Wb and 18.0×10^7 Wb, also considerably less than $(30–40) \times 10^7$ Wb of moderate substorms [*Pu et al.*, 2006]. The related solar wind input power ε' into the magnetosphere can be estimated as $\varepsilon' = \Psi_1^2 \times V_x/(\mu_0 S_T)$ [*Mishin and Falthammar*, 1998; *Mishin et al.*, 2001], here $\mu_0 = 4\pi \times 10^{-7}$ H, $S_T = 6 \times 10^{16}$ m^2 is a statistically empirical constant [*Mishin et al.*, 2001]. With $V_x \sim 380$ km/s (see Figure 2), we have $\varepsilon' \sim 2.4 \times 10^{11}$ W for the both substorms at AE maximums. For a comparison, Akasofu's lower threshold for a substorm power is 1.0×10^{11}W [*Akasofu*, 1977]. Obviously, these are consistent with the picture that tail lobe MR manifests the ultimate mechanism responsible for the main substorm expansion.

6. Summary

[23] THEMIS observations of two substorms on 26 February 2008 reveal that both were closely related to midtail MR and possess the following features:

[24] 1. A first, weak auroral intensification appeared about 1–2 min immediately after the midtail reconnection onset, followed by very limited poleward expansion of the arcs.

[25] 2. The second, major auroral intensification occurred (within about 1 min) when earthward flows and magnetic dipolarization were observed in the near-Earth tail; soon afterward the brightening region extensively expanded poleward.

[26] 3. During the growth phase of the substorms, the polar cap open magnetic flux accumulated; whereas in the expansion/recovery phase the polar cap open flux reduced quickly.

[27] 4. The AE index, west electrojet current, amplitudes of the negative H-bay and Pi2 pulsations were all less than those in moderate substorms. The MR rates in both events were close to the low limit of fast MR. The solar wind input

power into the magnetosphere, the polar cap open flux created by dayside merging and that released by tail lobe MR were all small in comparison with those for moderate substorms.

[28] These observations are in agreement with the assertion that tail reconnection initiates the initial pseudobreakup and the ensuing major expansion and releases and transports energy to eventually cause near-Earth dipolarization and the expansion phase onset of these two substorms.

[29] **Acknowledgments.** This work is supported by NSFC grants 40731056, 40974095, and 40904043 and the Chinese Major Research Project (grant 2006CB806305). THEMIS work in the U.S. was supported by NASA NAS5-02099. The fluxgate magnetometer team was supported by the Deutsches Zentrum für Luft- und Raumfahrt under grant 50QP0402. We acknowledge the Canadian Space Agency for support in fielding and data retrieval from the THEMIS GBO stations and for provision of data by the CARISMA network. The authors thank A. Viljanen (Image team), J. Posch (MACCS team), T. Iyemori (WDC-C2), K. Yumoto (Nagoya Univ.), O. Troshichev (AARI), D. Milling (CARISMA), E. Kharin (WDC-B), B. M. Shevtsov and A. Vinnitskiy (ICRRWP), the PIs of the projects INTERMAGNET, GIMA (Alaska Univ.), H. Gleisner (DMI, Copenhagen), S. Solovyev (ICRA SB RAS, Yakutsk), S. Khomutov (obs. Novosibirsk), and O. Kusonskiy (obs. Arti) for providing geomagnetic data. We thank H. Zhang for useful discussions and are grateful to A. Prentice and Judy Hohl for their help.

[30] Amitave Bhattacharjee thanks the reviewers for their assistance in evaluating this paper.

References

Akasofu, S.-I. (1977), *Physics of Magnetospheric Substorms*, D. Reidel, Dordrecht, Netherlands.

Angelopoulos, V. (2008), The THEMIS mission, *Space Sci. Rev.*, *141*, 5–34, doi:10.1007/s11214-008-9336-1.

Angelopoulos, V., et al. (2008), Tail reconnection triggering substorm onset, *Science*, *321*, 931–935, doi:10.1126/science.1160495.

Angelopoulos, V., et al. (2009), Response to comment on "Tail reconnection triggering substorm onset", *Science*, *324*, 1391, doi:10.1126/science.1168045.

Arzner, K., and M. Scholer (2001), Kinetic structure of the post plasmoid plasma sheet during magnetotail reconnection, *J. Geophys. Res.*, *106* (A3), 3827–3844, doi:10.1029/2000JA000179.

Auster, H. U., et al. (2008), The THEMIS fluxgate magnetometer, *Space Sci. Rev.*, *141*, 235–264, doi:10.1007/s11214-008-9365-9.

Baker, D. N., T. I. Pulkkinen, V. Angelopoulos, W. Baumjohann, and R. L. McPherron (1996), Neutral line model of substorms: Past results and present view, *J. Geophys. Res.*, *101*, 12,975–13,010, doi:10.1029/95JA03753.

Baker, D. N., et al. (2002), Timing of magnetic reconnection initiation during a global magnetospheric substorm onset, *Geophys. Res. Lett.*, *29*(24), 2190, doi:10.1029/2002GL015539.

Baumjohann, W. (2002), Modes of convection in the magnetotail, *Phys. Plasmas*, *9*(9), 3665–3667, doi:10.1063/1.1499116.

Boakes, P. D., S. E. Milan, G. A. Abel, M. P. Freeman, G. Chisham, and B. Hubert (2009), A statistical study of the open magnetic flux content of the magnetosphere at the time of substorm onset, *Geophys. Res. Lett.*, *36*, L04105, doi:10.1029/2008GL037059.

Cao, X., et al. (2008), Multispacecraft and ground-based observations of substorm timing and activations: Two case studies, *J. Geophys. Res.*, *113*, A07S25, doi:10.1029/2007JA012761.

Cowley, S. W. H., and M. Lockwood (1992), Excitation and decay of solar wind-driven flows in the magnetosphere-ionosphere system, *Ann. Geophys.*, *10*, 103–115.

Deng, X. H., H. Matsumoto, H. Kojima, T. Mukai, R. R. Anderson, W. Baumjohann, and R. Nakamura (2004), Geotail encounter with reconnection diffusion region in the Earth's magnetotail: Evidence of multiple X lines collisionless reconnection?, *J. Geophys. Res.*, *109*, A05206, doi:10.1029/2003JA010031.

Ge, Y. S., C. T. Russell, and T.-S. Hsu (2008), Implication of multiple dipolarization event near 9 R_E for the physics of substorms, *Adv. Space Res.*, *41*, 1243–1251, doi:10.1016/j.asr.2007.12.010.

Immel, T. J., J. D. Craven, and L. A. Frank (1997), Influence of IMF BY on large-scale decreases of O column density at middle latitudes, *J. Atmos. Sol. Terr. Phys.*, *59*(6), 725–737, doi:10.1016/S1364-6826(96)00099-5.

Kamide, Y., and S.-I. Akasofu (1974), Latitudinal cross section of the auroral electrojet and its relation to the interplanetary magnetic field polarity, *J. Geophys. Res.*, *79*, 3755–3771, doi:10.1029/JA079i025p03755.

Koskinen, H. E. J., R. E. Lopez, R. J. Pellinen, T. I. Pulkkinen, D. N. Baker, and T. Bosinger (1993), Pseudobreakup and substorm growth phase in the ionosphere and magnetosphere, *J. Geophys. Res.*, *98*, 5801–5813, doi:10.1029/92JA02482.

Liang, J., E. F. Donovan, W. W. Liu, B. Jackel, M. Syrjäsuo, S. B. Mende, H. U. Frey, V. Angelopoulos, and M. Connors (2008), Intensification of preexisting auroral arc at substorm expansion phase onset: Wave-like disruption during the first tens of seconds, *Geophys. Res. Lett.*, *35*, L17S19, doi:10.1029/2008GL033666.

Lui, A. T. Y. (1996), Current disruption in the Earth's magnetosphere: Observations and models, *J. Geophys. Res.*, *101*, 13,067–13,088, doi:10.1029/96JA00079.

Lui, A. T. Y. (2009), Comment on "Tail reconnection triggering substorm onset,", *Science*, *324*, 1391, doi:10.1126/science.1167726.

Lui, A. T. Y., S.-I. Akasofu, E. W. Hones Jr., S. J. Bame, and C. E. McIlwain (1976), Observation of the plasma sheet during a contracted oval substorm in a prolonged quiet period, *J. Geophys. Res.*, *81*, 1415–1419, doi:10.1029/JA081i007p01415.

Lui, A. T. Y., A. Mankofsky, C.-L. Chang, K. Papadopoulos, and C. S. Wu (1990), A current disruption mechanism in the neutral sheet: A possible trigger for substorm expansions, *Geophys. Res. Lett.*, *17*, 745–748, doi:10.1029/GL017i006p00745.

Manapat, M., M. Øieroset, T. D. Phan, R. P. Lin, and M. Fujimoto (2006), Field-aligned electrons at the lobe/plasma sheet boundary in the mid-to-distant magnetotail and their association with reconnection, *Geophys. Res. Lett.*, *33*, L05101, doi:10.1029/2005GL024971.

McFadden, J. P., C. W. Carlson, D. Larson, M. Ludlam, R. Abiad, B. Elliott, P. Turin, M. Marckwordt, and V. Angelopoulos (2008), The THEMIS ESA plasma instrument and in-flight calibration, *Space Sci. Rev.*, *141*, 277–302, doi:10.1007/s11214-008-9440-2.

McPherron, R. L. (1991), Physical processes producing magnetospheric substorms and magnetic storms, in *Geomagnetism*, vol. 4, edited by J. Jacobs, pp. 593–739, Academic, London.

McPherron, R. L. (2004), Substorms, paper presented at COSPAR Workshop on Capacity Development, Comm. on Space Res., Beijing, May. (Available at http://www.faculty.iu-bremen.de/jvogt/cospar/cbw3/substorms/lecture_rmcpherron.pdf.)

Mende, S. B., S. E. Harris, H. U. Frey, V. Angelopoulos, C. T. Russell, E. Donovan, B. Jackel, M. Greffen, and L. M. Peticolas (2008), The THEMIS array of ground-based observatories for the study of auroral substorms, *Space Sci. Rev.*, *141*, 357–387, doi:10.1007/s11214-008-9380-x.

Mishin, V. M. (1990), The magnetogram inversion technique and some applications, *Space Sci. Rev.*, *53*, 83–163, doi:10.1007/BF00217429.

Mishin, V. M., and C.-G. Falthammar (1998), Pseudo- and true substorm onsets within framework of the analogy "magnetospheric substorms-solar flares," in *Substorms-4*, edited by S. Kokobun and Y. Kamide, pp. 319–322, Terra Sci., Tokyo.

Mishin, V. M., et al. (1997), A study of the CDAW9C substorm, May 3, 1986, using magnetogram inversion technique 2, and a substorm scenario with two active phases, *J. Geophys. Res.*, *102*, 19,845–19,859.

Mishin, V., C. Russell, T. Saifudinova, and A. Bazarzhapov (2000), Study of weak substorms observed during December 8, 1990, Geospace Environment Modeling campaign: Timing of different types of substorm onsets, *J. Geophys. Res.*, *105*(A10), 23,263–23,276, doi:10.1029/1999JA900495.

Mishin, V. M., T. I. Saifudinova, A. D. Bazarzhapov, C. T. Russell, W. Baumjohann, R. Nakamura, and M. Kubyshkina (2001), Two distinct substorm onsets, *J. Geophys. Res.*, *106*(A7), 13,105–13,118, doi:10.1029/2000JA900152.

Mishin, V., L. Sapronova, T. Saifudinova, R. Lukianova, and Y. Kuzminykh (2008), The Hall's and Cowling's currents contribution into the westward auroral electrojet during substorm unloading phase, paper presented at "Physics of Auroral Phenomena," XXXI Annual Seminar, pp. 42–45, Kola Sci. Cent., Russian Acad. of Sci., Apatity, Russia.

Nagai, T., I. Shinohara, M. Fujimoto, M. Hoshino, Y. Saito, S. Machida, and T. Mukai (2001), Geotail observations of the Hall current system: Evidence of magnetic reconnection in the magnetotail, *J. Geophys. Res.*, *106*(A11), 25,929–25,949, doi:10.1029/2001JA900038.

Nakamura, R., D. N. Baker, T. Yamamoto, R. D. Belian, E. A. Bering III, J. R. Benbrook, and J. R. Theall (1994), Particle and field signatures during pseudobreakup and major expansion onset, *J. Geophys. Res.*, *99*(A1), 207–221, doi:10.1029/93JA02207.

Nakamura, R., W. Baumjohann, Y. Asano, A. Runov, A. Balogh, C. J. Owen, A. N. Fazakerley, M. Fujimoto, B. Klecker, and H. Rème (2006), Dynamics of thin current sheets associated with magnetotail reconnection, *J. Geophys. Res.*, *111*, A11206, doi:10.1029/2006JA011706.

Ohtani, S., et al. (1993), A multisatellite study of a pseudo-substorm onset in the near-Earth magnetotail, *J. Geophys. Res.*, *98*, 19,355–19,367, doi:10.1029/93JA01421.

Øieroset, M., T. D. Phan, M. Fujimoto, R. P. Lin, and R. P. Lepping (2001), In situ detection of collisionless reconnection in the Earth's magnetotail, *Nature*, *412*(6845), 414–417, doi:10.1038/35086520.

Owen, C. J., J. A. Slavin, A. N. Fazakerley, M. W. Dunlop, and A. Balogh (2005), Cluster electron observations of the separatrix layer during traveling compression regions, *Geophys. Res. Lett.*, *32*, L03104, doi:10.1029/2004GL021767.

Phan, T. D., et al. (2000), Extended magnetic reconnection at the Earth's magnetopause from detection of bi-directional jets, *Nature*, *404*, 848–850, doi:10.1038/35009050.

Priest, E. R., and T. Forbes (2000), *Magnetic Reconnection: MHD Theory and Applications*, Cambridge Univ. Press, Cambridge, U. K.

Pu, Z. Y., et al. (1999), Ballooning instability in the presence of a plasma flow: A synthesis of tail reconnection and current disruption models for the initiation of substorms, *J. Geophys. Res.*, *104*, 10,235–10,248, doi:10.1029/1998JA900104.

Pu, Z. Y., A. Korth, Z. X. Chen, Z. X. Liu, S. Y. Fu, G. Zong, M. H. Hong, and X. M. Wang (2001), A global synthesis model of dipolarization at substorm expansion onset, *J. Atmos. Sol. Terr. Phys.*, *63*, 671–681, doi:10.1016/S1364-6826(00)00183-8.

Pu, Z., et al. (2006), Observational features of magnetotail open field line reconnection, *Eos Trans. AGU*, *87*(52), Fall Meet. Suppl., Abstract SM44B-05.

Pu, Z. Y., et al. (2005), Double Star TC-1 observations of component reconnection at the dayside magnetopause: A preliminary study, *Ann. Geophys.*, *23*, 2889–2895.

Rostoker, G., S.-I. Akasofu, J. C. Foster, R. A. Greenwald, Y. Kamide, K. Kawasaki, A. T. Y. Lui, R. L. McPherron, and C. T. Russell (1980), Magnetospheric substorms—Definition and signatures, *J. Geophys. Res.*, *85*, 1663–1668, doi:10.1029/JA085iA04p01663.

Runov, A., et al. (2008), Multipoint in situ and ground-based observations during auroral intensifications, *J. Geophys. Res.*, *113*, A00C07, doi:10.1029/2008JA013493.

Russell, C. T. (2000), How northward turning of the IMF can lead to substorm expansion onsets, *Geophys. Res. Lett.*, *27*, 3257–3259, doi:10.1029/2000GL011910.

Russell, C. T., P. J. Chi, D. J. Dearborn, Y. S. Ge, B. Kuo-Tiong, J. D. Means, D. R. Pierce, K. M. Rowe, and R. C. Snare (2008), THEMIS ground-based magnetometers, *Space Sci. Rev.*, *141*, 389–412, doi:10.1007/s11214-008-9337-0.

Sergeev, V. A., S. V. Apatenkov, V. Angelopoulos, J. P. McFadden, D. Larson, J. W. Bonnell, M. Kuznetsova, N. Partamies, and F. Honary (2008), Simultaneous THEMIS observations in the near-tail portion of the inner and outer plasma sheet flux tubes at substorm onset, *J. Geophys. Res.*, *113*, A00C02, doi:10.1029/2008JA013527.

Shiokawa, K., W. Baumjohann, and G. Haerendel (1997), Braking of high-speed flows in the near-Earth tail, *Geophys. Res. Lett.*, *24*(10), 1179–1182, doi:10.1029/97GL01062.

Shiokawa, K., et al. (1998), High-speed ion flow, substorm current wedge, and multiple Pi 2 pulsations, *J. Geophys. Res.*, *103*(A3), 4491–4507, doi:10.1029/97JA01680.

Sonnerup, B. U. Ö., and M. Scheible (1998), Minimum variation analysis, in *Analysis Methods for Multi-Spacecraft Data*, edited by G. Paschmann and P. W. Daly, *ISSI Sci. Rep. SR-001*180–208, Int. Space Sci. Inst., Bern.

Speiser, T. W., R. F. Martin Jr., and N. Sckopke (1996), Bursty bulk flows, the geomagnetic tail current sheet, and substorm timing, *Adv. Space Res.*, *18*(8), 73–78, doi:10.1016/0273-1177(95)01000-9.

Tsyganenko, N. (1995), Modeling the Earth's magnetospheric magnetic field confined within a realistic magnetopause, *J. Geophys. Res.*, *100* (A4), 5599–5612, doi:10.1029/94JA03193.

Zhang, H., et al. (2007), TC-1 observations of flux pileup and dipolarization-associated expansion in the near-Earth magnetotail during substorms, *Geophys. Res. Lett.*, *34*, L03104, doi:10.1029/2006GL028326.

Zhou, X.-Z., V. Angelopoulos, A. Runov, M. I. Sitnov, Q.-G. Zong, and Z. Y. Pu (2009), Ion distributions near the reconnection sites: Comparison between simulations and THEMIS observations, *J. Geophys. Res.*, *114*, A12211, doi:10.1029/2009JA014614.

V. Angelopoulos, J. Liu, C. T. Russell, and X. Z. Zhou, IGPP, UCLA, Los Angeles, CA 90065-1567, USA.

X. Cao, X. N. Chu, S. Y. Fu, Z. Y. Pu, J. Wang, Y. Wei, L. Xie, and Q. G. Zong, School of Earth and Space Sciences, Peking University, Beijing 100871, China.

H. Frey, D. Larson, J. McFadden, and S. Mende, Space Sciences Laboratory, University of California, 7 Gauss Way, Berkeley, CA 94720, USA.

K.-H. Glassmeier, Institute for Geophysics and Extraterrestrial Physics, Technical University of Braunschweig, D-38106 Braunschweig, Germany.

E. Lucek, Blackett Laboratory, Imperial College, London SW7 2AZ, UK.

I. Mann, Department of Physics, University of Alberta, Edmonton, AB T6G 2J1, Canada.

V. Mishin, T. I. Saifudinova, L. A. Sapronova, and M. V. Tolochko, Institute of Solar-Terrestrial Physics, Russian Academy of Sciences, PO Box 4026, Irkutsk 664033, Russia.

H. Reme, Centre d'Etude Spatiale des Rayonnements, 9 Ave. Colonel-Roche, B. P. 4346,Toulouse F-31028, France.

D. Sibeck, NASA GSFC, Code 674, Greenbelt, MD 20771, USA.

X. G. Wang, C. J. Xiao, and Z. H. Yao, School of Physics, Peking University, Beijing 100871, China.